Photo-Patternable Hole-Transport Polymers for Organic Light-Emitting Diodes

Benoit Domercq,[†] Richard D. Hreha,[‡] Ya-Dong Zhang,[‡] Nathalie Larribeau,[†] Joshua N. Haddock,[†] Christopher Schultz,[†] Seth R. Marder,[†,‡] and Bernard Kippelen*[,†]

Optical Sciences Center and Department of Chemistry, University of Arizona, Tucson, Arizona 85721

A series of soluble arylamine-based hole transporting polymers with various ionization potentials have been synthesized. The synthetic methodology allows for substitution of aryl groups on the amine with electron-withdrawing and electron-donating moieties which permits tuning of the redox potential of the polymer. The arylamine-based monomers have been copolymerized with cinnamate-based moieties to obtain photo-cross-linkable polymers. These materials can be cross-linked and patterned using a standard mask aligner designed for photolithographic applications. UV cross-linking conditions were optimized to obtain an insoluble hole-transport layer with stable electroluminescent properties. Using a photolithographic mask, these materials have been patterned into 10−50-μm-size features. These polymers have been used as hole-transport layers (HTLs) in multilayer light-emitting diodes ITO/HTL/AlQ_3/Mg:Ag [ITO = indium tin oxide, AlQ_3 = tris(8-hydroxyquinolinato)aluminum]. The electroluminescent properties have been evaluated and compared between devices made from polymers with different ionization potentials. Electroluminescent devices have been fabricated using a multilayered structure of spin-coated hole-transport materials to enhance the overall electroluminescent properties. Fully spin-coated devices have also been fabricated by spinning a blend of polystyrene and AlQ_3 on top of a cross-linked hole-transport layer.

Introduction

Organic light-emitting diodes (OLEDs) are generally fabricated by deposition of multiple layers of materials.[1] High external efficiencies have been demonstrated recently using phosphorescent[2] and/or fluorescent dopants.[3] The preparation of multilayer structures from solution is difficult because the bottom layer can be dissolved upon application of a subsequent layer from solution. The utilization of precursor polymers and their thermal conversion into an insoluble film, well established, for instance, for poly(*p*-phenylenevinylene) (PPV),[4] circumvents this problem. However, this approach narrows the scope of materials that can be fabricated and patterned. An alternative approach is to photo-cross-link monomers[5−7] or pre-polymers[8−11] containing polymerizable moieties, either as side groups or in the main chain of the polymer, into an insoluble material. Generally, long UV exposure (between 5 min and 1 h),[7−9] the use of an in situ UV-generated photoacid,[6] or an additional thermal treatment step (using temperature up to 150 °C)[10,12] are required to cross-link the films. A significant decrease in the overall performance of devices made from these cross-linkable materials has generally been observed after cross-linking.[7,9] This may be due to the partial degradation of the transport molecules under long UV exposure and/or extended thermal treatment.

When the cross-linking is induced optically, the material not only becomes insoluble, but can simultaneously be patterned like a photoresist using standard photolithography techniques. Patterning of the material into pixels is an important step in the fabrication of displays. With small molecules, patterning can be achieved using shadow masking during the vacuum deposition process, but with polymers patterning has been more challenging and often requires the fabrication of barriers and pillars to contain the polymer in specific areas. Another advantage of using cross-linkable materials for OLED applications is the stability of the

* To whom correspondence should be addressed. Tel: 520 621-4341. Fax: 520 626-4221. E-mail: kippelen@u.arizona.edu.
[†] Optical Sciences Center.
[‡] Department of Chemistry.

(1) Tang, C. W.; VanSlyke, S. A. *Appl. Phys. Lett.* **1987**, *51*, 913.
(2) Baldo, M. A.; O'Brien, D. F.; You, Y.; Shoustikov, A.; Sibley, S.; Thompson, M. E.; Forrest, S. R. *Nature* **1998**, *395*, 151.
(3) D'Andrade, B. W.; Baldo, M. A.; Adachi, C.; Brooks, J.; Thompson, M. E.; Forrest, S. R. *Appl. Phys. Lett.* **2001**, *79*, 1045.
(4) Borroughes, J. H.; Bradley, D. D. C.; Brown, A. R.; Marks, R. N.; Mackay, K.; Friend, R. H.; Burns, P. L.; Holmes, A. B. *Nature* **1990**, *347*, 539.
(5) Li, W.; Wang, Q.; Cui, J.; Chou, H.; Shaheen, S. E.; Jabbour, G. E.; Anderson, J.; Lee, P.; Kippelen, B.; Peyghambarian, N.; Armstrong, N. R.; Marks, T. J. *Adv. Mater.* **1999**, *11*, 730.
(6) Bayerl, M. S.; Braig, T.; Nuyken, O.; Müller, D. C.; Gross, B.; Meerholz, K. *Macromol. Rapid Commun.* **1999**, *20*, 224.
(7) Zhang, Y.-D.; Hreha, R. D.; Jabbour, G. E.; Kippelen, B.; Peyghambarian, N.; Marder, S. R. *J. Mater. Chem.* **2002**, *12*, 1703.
(8) Li, X.-C.; Yong, T.-M.; Grüner, J.; Holmes, A.; Moratti, S.; Cacialli, F.; Friend, R. H. *Synth. Metals* **1997**, *84*, 437.
(9) Bellmann, E.; Shaheen, S. E.; Thayumanavan, S.; Barlow, S.; Grubbs, R. H.; Marder, S. R.; Kippelen, B.; Peyghambarian, N. *Chem. Mater.* **1998**, *10*, 1668.
(10) Braig, T.; Müller, D. C.; Gross, B.; Meerholz, K.; Nuyken, O. *Macromol. Rapid Commun.* **2000**, *21*, 583.
(11) Klärner, G.; Lee, J. I.; Lee, V. Y.; Chan, E.; Chen, J. P.; Nelson, A.; Markiewicz, D.; Siemens, R.; Scott, J. C.; Miller, R. D. *Chem. Mater.* **1999**, *11*, 1800.
(12) Bacher, A.; Erdelen, C. H.; Paulus, W.; Ringsdorff, H.; Schmidt, H.-W.; Schumacher, P. *Macromolecules* **1999**, *32*, 4551.

10.1021/cm020862u CCC: $25.00
Published on Web 03/15/2003

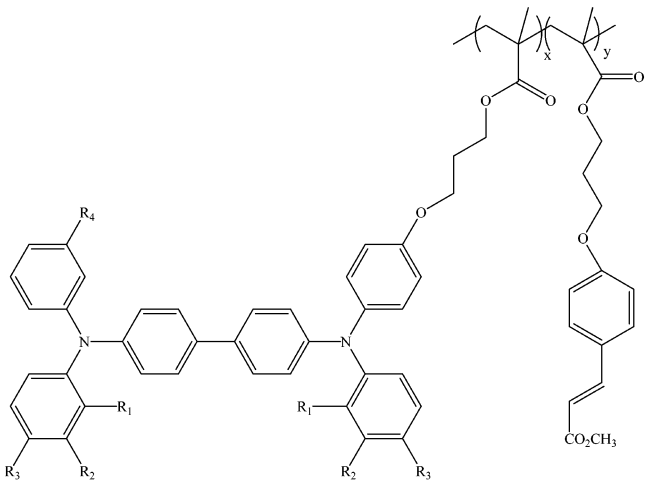

Figure 1. Structure of the cross-linkable TPD-based copolymers (with $x = 0.7$ and $y = 0.3$).

Table 1. Substituents of the Different TPD-Based Co-polymers

polymer	R1	R2	R3	R4
P1	H	Me	H	H
P2	H	H	OMe	Me
P3	H	F	H	Me
P4	F	H	F	Me

morphology of the films under thermal stress after cross-linking. For instance, some cross-linked films based on oxetane-functionalized bis(diarylamine) derivatives have been shown to exhibit good phase stability after cross-linking for temperatures up to 250 °C with no degradation of the film.[6] The thermal stability of the transport layers for OLEDs applications has been the focus of a recent study[13] because it has been suggested that poor device lifetimes are partially due to the limited thermal stability of the amorphous organic layers, even for devices operating at normal temperatures.[14,15] Therefore, the use of cross-linkable materials could be a way to obtain thermally stable layers and, eventually, devices with improved lifetimes.

Here, we describe the use of a series of photo-cross-linkable acrylate hole-transport polymers, based upon copolymerization of substituted bis(diarylamino)biphenyl acrylate monomers and cinnamate acrylate monomers, that undergo cross-linking under UV light exposure through a 2 + 2 cycloaddition. The polymers **P1**, **P2**, **P3**, and **P4** synthesized for this study are summarized in Table 1 and the general structure of the copolymer is shown in Figure 1. An advantage of using a copolymer approach is that the material can be easily processed from solution into a pinhole-free thin film. Also, the ratio of cross-linking monomers and transport monomers can easily be adjusted and optimized. Furthermore, the small shrinkage associated with the cross-linking process may reduce the number of pinholes that can be created during the coating process, reducing the leakage currents of the device when operating at low voltages. The substitution of the aryl groups on the amine with electron-withdrawing or electron-donating moieties allows for the tuning of the redox potential of the polymer. This tuning is important to optimize both the energy difference between the anode and the highest occupied molecular orbital (HOMO) of the hole-transport layer (to control hole injection), and the efficiency of the cross reaction between the radical cation of the hole-transport material and the radical anion of the electron-transport material that leads to the formation of luminescent excited states.

The paper is organized as follows. We first describe the properties of four different copolymers with various ionization potentials, and discuss the cross-linking properties of these layers. We show that their processing is compatible with a standard mask aligner used for photolithography and does not require additional thermal treatment. The thermal stability of the morphology of the cross-linked polymer films is studied by optical microscopy and atomic force microscopy (AFM) and compared to vapor-deposited N, N′-bis-(*m*-tolyl)-N,N′-diphenyl-1,1′-biphenyl-4,4′-diamine (TPD) small-molecule films. Then, we present the electrical and photometric properties of OLEDs that were fabricated using these polymers spin-coated from solution as hole-transport layers (HTL) in conjunction with vapor-deposited AlQ_3 as an electron-transport/emissive layer, and Mg:Ag as a cathode. First, we describe the performance of OLED devices with a single hole-transport layer fabricated from non cross-linked polymers and compare their properties to devices in which the hole-transport layer was cross-linked under various UV exposure conditions. Next, we discuss the performance of devices with two cross-linked hole-transport layers. This leads to an enhancement of the external quantum efficiency. We also describe a device in which a single cross-linked hole-transport layer is overcoated by a polymeric layer composed of AlQ_3 doped into polystyrene. In this device both layers are based on well-know molecular building blocks used in the small-molecule approach, but in this case they are processed from solution as in the polymer approach. Finally, we study the effects of cross-linking on the operational lifetime of the device at constant current and compare this lifetime to that of small-molecule devices fabricated with evaporated TPD and AlQ_3 molecules.

Experimental Section

Cross-Linking. The materials were cross-linked with a standard mask aligner using the 350-nm line of a mercury arc lamp with a 12 mW/cm^2 power density.

Device Fabrication. Films of 50−60-nm thickness were prepared by spin coating **P1**, **P2**, **P3**, or **P4** onto oxygen-plasma-treated ITO with a sheet resistance of 20 Ω/□(Colorado Concept Coatings, LLC) from toluene. Electron-transport layers composed of 60-nm-thick AlQ_3 films were thermally evaporated at a rate of 1 Å/s under a pressure of 1×10^{-6} Torr on top of the hole-transport layer. The metal cathode, an alloy of silver and magnesium in a 1 to 10 ratio, was deposited through a shadow mask to define five devices with an emissive area of 0.1 cm^2 each. For optical microscopy and AFM studies, TPD was evaporated at a rate of 1 Å/s under a pressure of 1×10^{-6} Torr.

Results and Discussion

Material and Single Film Characterization. The synthesis of this new series of photo-cross-linkable

(13) Loy, D. E.; Koene, B. E.; Thompson, M. E. *Adv. Func. Mater.* **2002**, *12*, 245.
(14) Fenter, P.; Schreiber, F.; Bulovic, V.; Forrest, S. R. *Chem. Phys. Lett.* **1997**, *277*, 521.
(15) Smith, P. F.; Gerroir, P.; Xie, S.; Hor, A.; M. Popovic, Z. *Langmuir* **1998**, *14*, 5946.

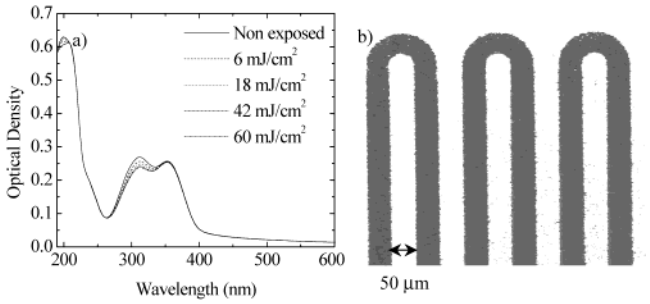

Figure 2. (a) Evolution of the absorption spectra of a 50-nm-thick film of **P3** under UV exposure. (b) Photograph of a set of 50-μm-size features obtained after photo-cross-linking (25 mJ/cm^2) and developing a 60-nm thin film of **P2**.

acrylate hole-transport polymers based upon copolymerization of substituted bis(diarylamino)biphenyl acrylate monomers (TPD monomers) and cinnamate acrylate monomers have been described elsewhere.[16] The copolymers contain 70 mol % of substituted TPD monomers and 30 mol % of cinnamate-substituted acrylate monomers (Table 1 and Figure 1). Each of the polymers is readily soluble in common organic solvents including THF, chloroform, toluene, benzene, and dichloromethane. The glass-transition temperatures (T_g) of the polymers before crosslinking were determined by differential scanning calorimetry (DSC). The glass-transition temperatures of polymers **P1**, **P2**, **P3**, and **P4** are 108, 97, 99, and 97 °C, respectively. There was no evidence of other thermal processes in the temperature range investigated (from 25 to 250 °C), suggesting that the polymers prepared were amorphous. The electrochemical properties such as the ionization potential of the polymer, can be tuned without changing drastically the bulk properties of the film. Indeed, these small changes did not appear to affect the film-forming properties of the polymer.

These TPD-based copolymers could be photo-cross-linked using the UV radiation (350 nm) provided by a standard UV-mask aligner through a 2 + 2 cycloaddition. To investigate the possible damage caused during UV cross-linking, we measured the absorption spectra of a thin film as a function of exposure to the UV light source. Figure 2a shows that the absorption band characteristic of the TPD group at 353 nm does not vary upon UV exposure, whereas the cinnamate absorption band at 312 nm decreases as a function of UV exposure. To efficiently cross-link the polymer, a minimum of 20 mJ/cm^2 of UV exposure is required. Although the extent of cross-linking is not known quantitatively at this exposure, it was sufficient to render the layer insoluble. We have been able to use standard lithographic equipment to pattern these materials and to define features in sizes ranging from 10 to 50 μm using a standard photolithography mask. An example of 50-μm-wide lines is shown in Figure 2b. To produce these features the polymer was spin-coated from toluene onto a glass substrate and exposed to UV light through the lithographic mask. Development was performed in a toluene solution for about 1 min.

In addition to providing for the possibility to pattern these films with UV light, cross-linking also has the advantage of transforming the polymer into a robust three-dimensional network of interconnected chains with high stability. The stability of the morphology of the cross-linked thin films under thermal stress has been investigated and compared to that of an evaporated TPD thin film. Films of **P2** or TPD with a thickness of 50 nm were spin-coated or vapor deposited, respectively, on top of fresh oxygen-plasma-treated ITO glass substrates. The polymer samples were cross-linked with a UV exposure of 25 mJ/cm^2. The evaporated TPD samples and the **P2** samples were heated at 80 °C and 150 °C, respectively, for 10 min on a hot plate at ambient atmosphere. In the case of the TPD films, a temperature of 80 °C is well above the glass-transition temperature of around 65 °C. In the case of the polymer, the temperature was chosen to be above the glass transition temperature of the un-cross-linked film. Although the glass-transition temperatures of the un-cross-linked materials are around 100 °C, the materials after cross-linking did not exhibit any glass-transition temperature. Figure 3a and b show optical microscopy images of vapor-deposited TPD films before and after annealing. The samples made with TPD small molecules exhibit catastrophic de-wetting/de-cohesion. On the other hand, the thermal treatment does not affect the cross-linked materials and no changes have been observed before and after annealing. AFM images taken over up to 10-μm length scales showed that the structure of the film is unchanged and neither is its uniformity. For instance, the roughness of the film before thermal treatment (0.319 nm (rms)) remains comparable after thermal treatment (0.251 nm (rms)). For comparison purposes, the samples made with TPD small molecules have a roughness of 0.924 nm (rms) before thermal treatment and become smoother after the thermal treatment (0.180 nm (rms)). The morphology of the cross-linked materials is therefore very stable under thermal stress.

Device Fabrication and Testing. *Studies on Un-Cross-Linked Polymer Layers.* To investigate the performance of these hole-transport polymers (**P1**, **P2**, **P3**, and **P4)** in device geometry, we fabricated OLEDs with the following structure: ITO/**Pn** (**n** = 1 to 4)/AlQ_3/MgAg. In first studies, the hole-transport polymers were un-cross-linked and the devices were protected from UV exposure. The green emitter AlQ_3 was chosen as an electron-transport and emitting material because its performance, when combined with TPD based hole-transport materials, is well documented.

OLED devices using these new polymers exhibit external quantum efficiencies comparable to those of their fully evaporated equivalents with maximum values above 1% (number of photons/electrons) for an applied voltage below 8 V. The light emission of all the devices corresponds to the typical AlQ_3 emission spectrum centered at 518 nm. Figure 4 shows the electrical and optical characteristics of an ITO/**P3**/AlQ_3/Mg:Ag device. The current density exhibits a typical diode behavior with a strong rectification with an applied voltage above 2 V. The light is first detected with our setup at 3 V when the luminance reaches 8 cd/m^2. Here, using **P3**, the external quantum efficiency reaches a maximum value of 1.2% at around 8 V and a luminance of 3490 cd/m^2 at a current of 100 mA/cm^2. The current in these devices could be recorded over 7 orders of

(16) Zhang, Y.-D.; Hreha, R. D.; Domercq, B.; Larribeau, N.; Haddock, J. N.; Kippelen, B.; Marder, S. R. *Synthesis* **2002**, 1201.

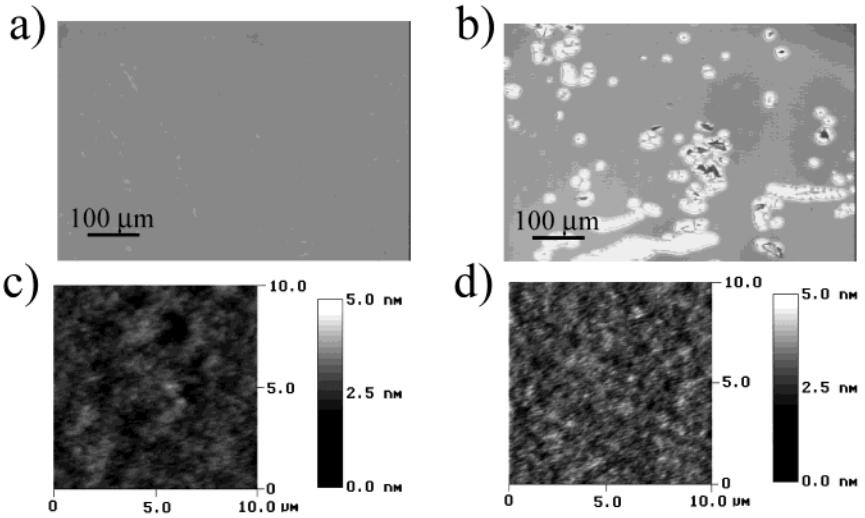

Figure 3. Optical microscopy images of vapor-deposited TPD films (60 nm) (a) before annealing and (b) after annealing at 80 °C for 10 min; and AFM image of **P2** thin films (50 nm) after cross-linking (c) before annealing and (d) after annealing at 150 °C for 10 min.

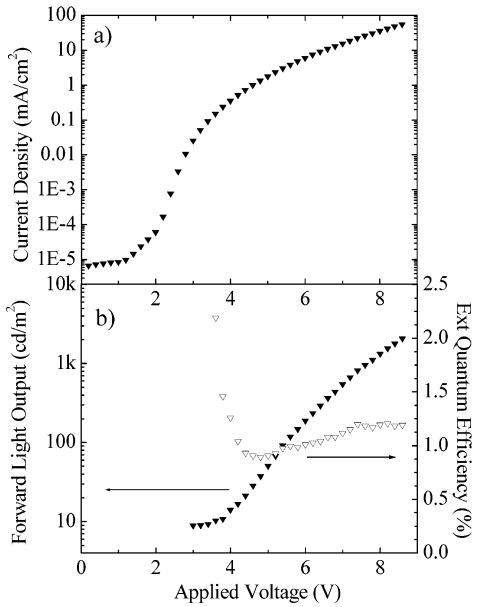

Figure 4. (a) Current density and (b) luminance and external quantum efficiency as a function of applied voltage for device with structure ITO/**P3**/AlQ_3/Mg:Ag (50 nm/50 nm/300 nm (10:1)).

magnitude. Note that a large proportion of the devices that were fabricated did not show leakage currents at low voltages, indicating that the polymer films have a good quality.

To study the effects of the ionization potential of the hole-transport layer on overall device performance, we fabricated devices with the general structure ITO/**Pn**/AlQ_3/Mg:Ag (10:1), in which **Pn** was one of the four unexposed hole-transport polymers **P1**, **P2**, **P3**, and **P4**. Table 2 summarizes the values of the halfwave oxidation potential measured by cyclic voltammetry and the corresponding estimated values of the ionization potential of the different polymers. The ionization potentials were estimated by considering the oxidation potentials relative to the reference ferrocenium/ferrocene redox couple and by assuming that the ionization potential of ferrocene relative to vacuum is 5.15 eV. These values of ionization potentials are admittedly approximate. Their main purpose is to provide for a simple way to compare the relative oxidation properties of different materials. For their accurate determination, photoemission spectroscopies in the solid state should be performed. The value of the ionization potential for each polymer has an impact on device performance as reported previously.[17,18] Increasing the ionization potential of the hole-transport layer was found to improve the external quantum efficiency because the driving force for the formation of excited states from a radical cation of the hole-transport material and a radical anion of the emitting material (AlQ_3 in our case) increases with the ionization potential of the hole-transport material. The trend observed in this study in the device efficiency as a function of the ionization potential of the hole-transport polymer is fully consistent with previous studies performed in poly(vinyl)TPD-type homopolymers with various ionization potentials.[17] The device with polymer **P3** shows the highest efficiency. As in the homopolymer case, devices based on the more highly fluorinated material (in this case, **P4**) deviate from this trend and have lower external quantum efficiency than the less fluorinated materials (here **P3**). This behavior is attributed to the limited stability of the compound itself.

As shown in Figure 5, all devices have similar "turn-on" voltages (around 2 V). This is the voltage that is required to reach the flat band condition in the device to compensate for the build-in field that results from the difference in work function between the electrodes and the difference between the frontier orbital energies of the hole- and electron-transport layers. This voltage appears to stay constant for the different devices because the resolution for its determination from the current/voltage characteristics is of the order of the

(17) Bellmann, E.; Shaheen, S. E.; Grubbs, R. H.; Marder, S. R.; Kippelen, B.; Peyghambarian, N. *Chem. Mater.* **1999**, *11*, 399.

(18) Anderson, J. D.; McDonald, E. M.; Lee, P. A.; Anderson, M. L.; Ritchie, E. L.; Hall, H. K.; Hopkins, T.; Padias, A.; Thayumanavan, S.; Barlow, S.; Marder, S. R.; Jabbour, G. E.; Shaheen, S. E.; Kippelen, B.; Peyghambarian, N.; Wightman, R. M.; Armstrong, N. R. *J. Am. Chem. Soc.* **1999**, *120*, 9646.

Table 2. Oxidation Potentials of the Various Un-Cross-linked Hole-Transport Polymers and Device Characteristics for Devices with the Structure ITO/Pn/AlQ_3/Mg:Ag

HTL	$E_{1/2}$[a] (mV) (I_p (eV)[b])	ext. quantum efficiency @ 100 mA/cm^2 (% photon/e$^-$)	light output @ 100 mA/cm^2 (cd/m^2)	applied voltage @ 100 mA/cm^2 (V)
P2	105 (5.25 eV)	0.6	1790	9.7
P1	190 (5.34 eV)	0.7	2100	10.1
P3	300 (5.45 eV)	1.1	3490	9.4
P4	320 (5.47 eV)	0.8	2360	9.4

[a] First oxidation potential measured vs the ferrocenium/ferrocene couple in dichloromethane. [b] I_p estimated from $E_{1/2}$ using ferrocenium/ferrocene-ion couple ($E°$ = 0.65 V) as internal standard. I_p (eV) = $E_{1/2}$ (V) + $E°$ (Fc^+/Fc) + 4.5

Table 3. Performance of OLED Devices with Structure ITO/P2/(P1 or P3)/AlQ_3/Mg:Ag (30 nm/30 nm/50 nm/300 nm (10:1)).

	applied voltage (V)	ext. quantum efficiency (%)	luminance (cd/m^2)	current density (mA/cm^2)	power efficiency (lm/W)
P2/P1	5.0	1.1%	52	1.5	2.1
	8.0	1.2%	685	18.3	1.5
P2/P3	5.0	1.3%	50	1.3	2.5
	8.0	1.4%	1409	32.4	1.7

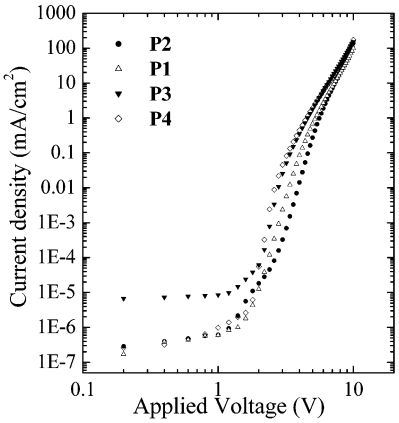

Figure 5. Current density as a function of applied voltage for devices with structure ITO/**P*n*** (***n*** = 1−4)/AlQ_3/Mg:Ag (50 nm/50 nm/300 nm (10:1)). In each device a different un-cross-linked polymer was used as hole-transport layer.

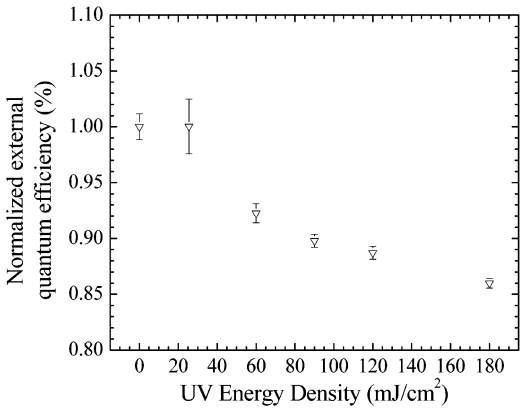

Figure 6. External quantum efficiency as a function of the UV energy density for devices with structure ITO/**P3**/AlQ_3/Mg:Ag (50 nm/50 nm/300 nm (10:1)).

tuning range of the ionization potential of the polymer layer.

Studies on Cross-Linked Polymer Layers. Upon cross-linking, we have previously found that the performance of OLEDs devices tends to decrease significantly.[7,9] Optimization of UV exposure is therefore critical for device performance. We have investigated the dependence of the device performance as a function of the UV exposure for devices with structure ITO/**P3**/AlQ_3/Mg:Ag. For each device, the hole-transport polymer was spin-coated and cross-linked using different UV energy densities ranging from 0 to 180 mJ/cm^2. The AlQ_3 layer was then deposited on all the samples during the same deposition run. Figure 6 shows the evolution of the external quantum efficiency as a function of the UV exposure energy density. For UV exposure energies of up to 25 mJ/cm^2 (which corresponds to an exposure time of less than 3 s on a standard mask aligner) the performance of the device is stable. This dose was also found to be sufficient to provide good cross-linking to enable the development of lithographically defined patterns (Figure 2b) and the fabrication of multilayer devices as discussed in the section below. No additional thermal treatment is required to achieve the cross-linking of the polymer.

Using this protocol, devices composed of multiple spin-coated layers were fabricated. As discussed above, the addition of an electron-attracting group like fluorine on TPD leads to more efficient devices. On the other hand, an increase of the ionization potential implies that the barrier for hole-injection at the anode is increased. To overcome these difficulties we fabricated devices with two hole-transport layers processed from solution. The low-ionization-potential polymer **P2** was spin coated first and cross-linked on top of an ITO substrate to optimize hole injection. Higher-ionization-potential polymers **P3** or **P1** were then spin-coated and cross-linked to enhance the efficiency of light emission. AlQ_3 (50 nm) was evaporated on top of the polymers and followed by the metal cathode (Mg:Ag). The overall performance was enhanced as summarized in Table 3. In both cases we see an increase of the external quantum efficiency, as well as of the light output. At an applied voltage of 8 V, the external quantum efficiency for a device using the combination of **P2/P1** peaks at 1.2% compared to 0.65 and 0.85% using single layers of **P2** or **P1**, respectively.

Finally, a fully spin-coated device was fabricated using a blend of polystyrene and AlQ_3 (PS:AlQ_3, 1:4) as the electron-transport and emissive material. The structure of the device is ITO/**P2/P3**/PS:AlQ_3/Mg:Ag (30 nm/30 nm/80 nm (1:4)/300 nm (10:1)). Figure 7 shows the performance of such devices. The current density pre-

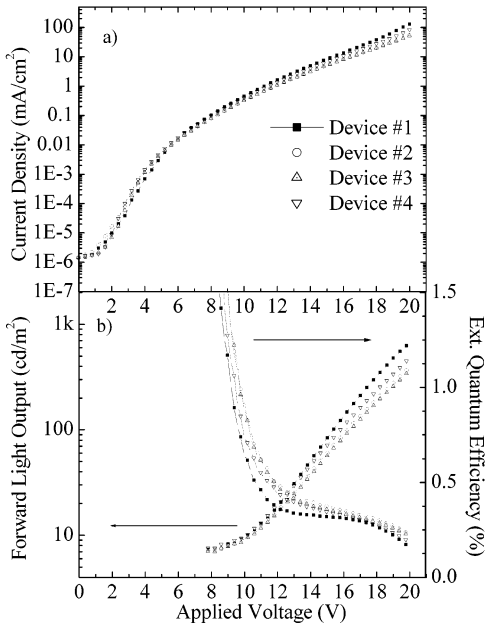

Figure 7. (a) Luminance and external quantum efficiency, and (b) current density, as a function of applied voltage for four devices with the structure ITO/**P2**/**P3**/PS:AlQ_3/Mg:Ag (30 nm/30 nm/80 nm (1:4)/300 nm (10:1)).

sents a typical diode behavior with a rectification above 2 V. However, the rectification is much weaker than that in the evaporated devices. The first light detected is at 8 V and the light output peaks at 600 cd/m^2 at 20 V. The current density is also much lower than that for the evaporated devices. This can be attributed to the lower mobility of the electron-transport layer PS:AlQ_3 compared to evaporated neat films of AlQ_3. The overall performance is then lower than the evaporated equivalent. Note the fairly good reproducibility of the device performance.

After cross-linking, the films are not only insoluble but also gain in morphology stability as discussed above. Morphology changes under thermal stress have been pointed out to be in part responsible for premature failure of devices based on small molecules with low glass-transition temperatures.[12−14] OLED materials are subjected to thermal stress in particular during device operation due to Joule heating. Crystallization and dewetting of the hole-transport layer have been observed after an extended period of device operation. One way to overcome these difficulties is to increase the glass-transition temperature (T_g) of the HTL. Recent work has shown that if the T_g of the HTL is increased, the operating temperature of the device increases.[12] However, no data on the lifetime of those devices have been reported.

To evaluate the influence of cross-linking of the hole-transport polymer on the operational stability of an OLED device, we performed lifetime measurements on a series of devices ITO/HTL/AlQ_3/Mg:Ag (10:1) at constant current densities of 50 mA/cm^2. These measurements were carried out in air. The light output and the voltage drop across the device were measured as a function of time. For devices fabricated with single layers of **P1**, **P2**, **P3**, and **P4** the half-lifetimes were 681, 1575, 1849, and 140 s, respectively. The devices fabricated with the polymer **P3** were the most stable. Note that significant differences in lifetimes are observed despite the fact that all polymers were cross-linked into a stable network. For comparison, lifetime measurements were also performed on devices with an un-cross-linked single layer of **P2**. Such devices yielded half-lifetime values (1550 s) comparable to those fabricated with a cross-linked layer of **P2**. We also performed lifetime experiments in similar conditions on devices with structure ITO/**P2**/**P1**/AlQ_3/Mg:Ag. The device with multiple hole-transport layers yielded a half-lifetime of 1208 s, a value comparable to that of devices fabricated with a single layer of **P2**. At the half-lifetime, the drive voltage of the device with two transport layers was increased by 6.9% compared to the initial voltage. Finally, we conducted such lifetime experiments on fully vapor-deposited devices with structure ITO/TPD/AlQ_3/Mg:Ag (50 nm/50 nm/250 nm (10:1)). Surprisingly, these devices yielded half-lifetimes values of 36000 s (10 h), much higher than those of any of the devices with polymeric hole-transport layers. In these devices, the increase in drive voltage at the half-lifetime was only 0.5%. This study shows that although cross-linking provides layers with a stable morphology, other factors do significantly impair the operational lifetime of OLED devices based on these new materials.

Conclusions

A new series of hole-transport materials based on triarylamines with cross-linkable cinnamate moieties has been successfully prepared. These polymers have been patterned using standard photolithographic techniques to obtain features from 10 to 50 μm in size. By using different substituents, the ionization potential could be tuned. The performance of these hole-transport materials in multilayer OLEDs was studied. The dependence of the external quantum efficiency on the ionization potential of these new copolymers was consistent with that reported previously in poly(vinyl)TPD-type homopolymers with various ionization potentials.[17] By optimizing the UV exposure dose, no loss in device efficiency was observed upon cross-linking of the hole-transport polymer. A maximum device efficiency of 1.4% could be achieved by using two spin-coated hole-transport polymer layers with different ionization potential. With these materials, fully spin-coated devices using a blend of polystyrene and AlQ_3 as electron-transport and emitter material could be fabricated. Despite high morphology stability in the cross-linked materials, the operational lifetime at constant current of polymer-based devices was found to be inferior to that of their counterparts fabricated by physical vapor deposition.

Acknowledgment. This work was partially funded by NSF through a CAREER grant (B.K.), by ONR, by NASA through the University of Alabama at Huntsville, by Durel Corp., and by the State of Arizona through Proposition 301 Initiative. We would like to thank Chet Carter for his help for the AFM studies.

CM020862U